

Experimental study on the shear capacity of randomly-cracked longitudinally-reinforced FRC beams

T. Miki, I.O. Toma & J. Niwa

Department of Civil Engineering, Tokyo Institute of Technology, Tokyo, Japan

ABSTRACT: This study is aimed at investigating the influence of steel fibers on the shear behavior of RC beams with random cracks. Since obtaining randomly-cracked concrete elements takes a lot of time and special conditions, the use of an expansion agent came as a solution to have extensive cracking. The idea of using short fibers came from the well-known fact that they behave very well as crack arrestors. Strain gages were attached to the longitudinal steel bars to monitor the strain variation during the curing process. At the same time, concrete surface strains were monitored and recorded by a data logger. Four-point loading tests were carried out on the RC beams. Steel fibers proved to be effective in reducing the overall expansion of the beams. An increase in the shear carrying capacity and deformability of the beams with steel fibers was observed.

1 INTRODUCTION

Many studies have been carried out to analyze and understand the shear failure of RC beams (Bresler & Scordelis 1963, Kreffeld & Thurston 1966). This type of failure is due to the combined action of shear and flexure and may happen in a brittle way, without any warning signs. The shear carrying capacity of RC beams can greatly decrease when the concrete members are already cracked. Cracks can appear in concrete members due to a multitude of factors either external (severe environment, loads) or internal (chemical reactions within concrete). Engineers have looked for ways to improve concrete properties and behavior and for ways to protect it from these attacks but their efforts were not always successful.

One of the undesired phenomena occurring in concrete structures is random cracking. There are many causes leading to random cracking and one of them is Alkali Silica Reaction (ASR). Many studies have been performed in order to better understand ASR (Smaoui et al. 2005). The basics of ASR consist in the formation of ASR gel which swells, provided that enough moisture is present, creating tensile stresses in the surrounding cement matrix. When the induced tensile stresses become larger than the tensile strength of the matrix, cracking occurs. As a result of the improved understanding of ASR, methods have been developed and proposed to either slow down or completely avoid it. However, some of these methods gave unexpected results on the long run (Diamond 1997). For example, it was found out

that silica fume can induce ASR rather than mitigating it (Petersen 1992).

2 RESEARCH MOTIVATION AND OBJECTIVES

While most of today's research in the field of concrete focuses on the properties and behavior of undamaged concrete elements, the present research aims at investigating the shear resistance of RC beams affected by random cracking. Moreover, the possible use of short steel fibers as a tool to improve the behavior of randomly-cracked concrete beams is also studied.

Thus, the objectives are: to create random cracks in RC beams, to investigate the role of steel fibers in RC beams with random cracks and to understand the shear behavior of steel fiber-reinforced concrete beams with random cracks.

Because obtaining random cracking in a concrete specimen requires a long time and special conditions, the use of an expansion agent came as a solution to have extensive cracking. Expansion agents, also known as shrinkage reducing admixtures, are special products developed to increase the volume of concrete by means of specific chemical reactions. According to the literature (Colleparidi et al. 2005) there are two main types of expansion agents: those based on ettringite formation and those based on the formation of calcium hydroxide. In this study, an expansion agent of the second type was used.

Table 1. Mix proportions for each of the concrete batches.

Concrete Type	W* ¹ [kg/m ³]	C* ² [kg/m ³]	W/C [%]	S* ³ [kg/m ³]	G* ⁴ [kg/m ³]	EA* ⁵ [kg/m ³]	F* ⁶ [kg/m ³]	AE* ⁷ [kg/m ³]	SP* ⁸ [kg/m ³]
C	175	350	50	788	963	-	-	2.8	1.75
0F95EA	175	350	50	708	963	95	-	2.8	1.75
05F102EA	175	350	50	702	963	102	40	2.8	2.6
05F110EA	175	350	50	695	963	110	40	2.8	2.6
10F110EA	175	350	50	692	963	110	80	2.8	2.6
10F130EA	175	350	50	679	963	130	80	2.8	2.6

*1 Water, *2 early strength Portland Cement, specific gravity = 3.14, *3 Fine aggregate, specific gravity = 2.64, *4 Coarse aggregate, specific gravity = 2.64, d_a (maximum aggregate size) = 20 mm, *5 Expansion agent, specific gravity = 3.14, *6 Steel fibers, specific gravity = 7.85, *7 Air entraining agent, specific gravity = 1.03, *8 Superplasticizer, high performance water reducing agent, specific gravity = 1.05.

Table 2. Properties of concrete.

Concrete Type	f'_c * ¹ [N/mm ²]	f_t * ² [N/mm ²]
C	34.8	2.4
0F95EA	2.7	0.2
05F102EA	4.9	0.5
05F110EA	2.5	0.3
10F110EA	8.9	1.1
10F130EA	2.2	0.3

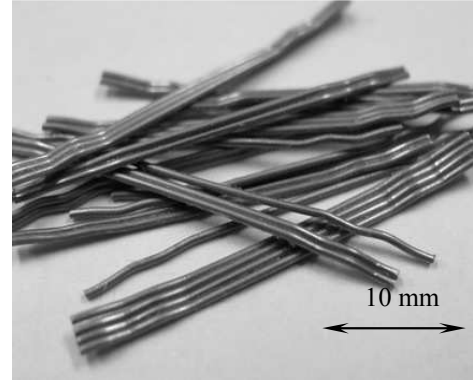


Figure 1. Steel fibers layout.

(nominal diameter: $d = 25.4 \mu\text{m}$) and steel grade SD345 (yield strength: $f_y = 345 \text{ N/mm}^2$). The specifications are according to JIS G 3112.

3.3 Steel fibers

The steel fibers have crimped ends as it can be seen from Figure 1. The length is $L_f = 30 \text{ mm}$ and the diameter is $d_f = 0.6 \text{ mm}$. The material properties are: the tensile strength $f_u = 1000 \text{ N/mm}^2$ and the Young's modulus $E = 2.1 \times 10^5 \text{ N/mm}^2$.

3.4 Expansion agent

The amount of expansion agent was chosen in order to replace a part of the fine aggregate mass and not of the cement mass. This was based on the fact that with the quality control commonly achieved in modern cement factories, the flaws are more likely to come from the aggregates that are used in the mixing than from the cement itself. Moreover, in some damaging processes like ASR, the silica in the aggregate reacts with the alkali in the cement to create the ASR gel. Thus, the expansion agent stands for the reactive fine aggregate.

4 TEST PROGRAM

The test program consisted in a total number of six specimens. For each concrete mix in Table 1 a beam with the dimensions of $1200 \times 200 \times 150 \text{ mm}$ (L x H

*1 compressive strength of concrete obtained according to JIS 1108.

*2 tensile strength of concrete obtained according to JIS 1113.

Random cracks can hardly be controlled by using conventional reinforcement. On the other hand, the randomly-distributed steel fibers ensure a better control of cracking in any direction inside the concrete mass.

3 MATERIALS

3.1 Concrete

In this study, a concrete with a designed compressive strength of 30 N/mm^2 , obtained from uniaxial compression tests at 7 days, was considered. In view of the fact that early-strength Portland cement was used in the concrete mixes and taking into account the standard specifications for concrete structures in Japan (JSCE 2002) the uniaxial compressive tests could be run at 7 days and not at 28 days. The early strength Portland cement allows for a rapid development of concrete strength within the first 7 days. After that, the rate of increase in concrete strength is lower than that for normal Portland cement concrete. Six different mix proportions were considered and they are presented in Table 1. The compressive and tensile strengths of each of the concrete mixes were measured at the day of testing and they are summarized in Table 2.

3.2 Reinforcement

The characteristics of the conventional reinforcement used in this study are as follows: bar size D25

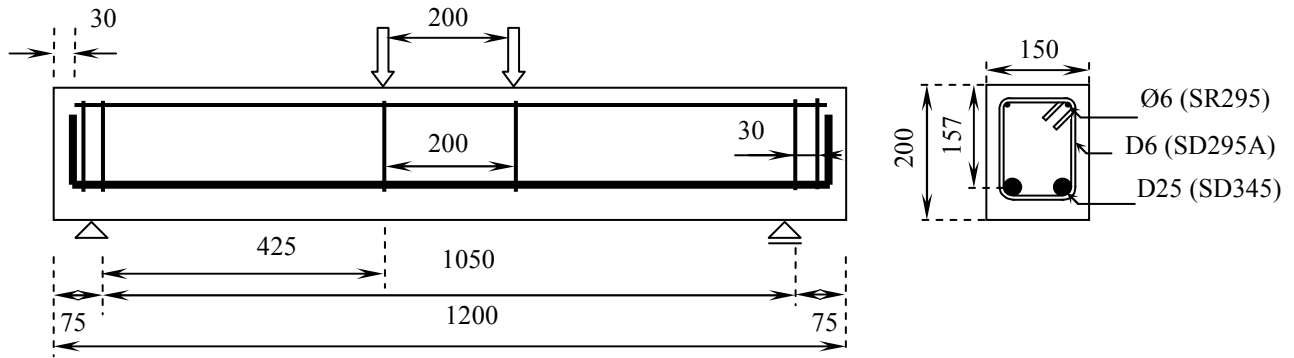


Figure 2. Beam geometry and reinforcement layout (all dimensions are in mm).

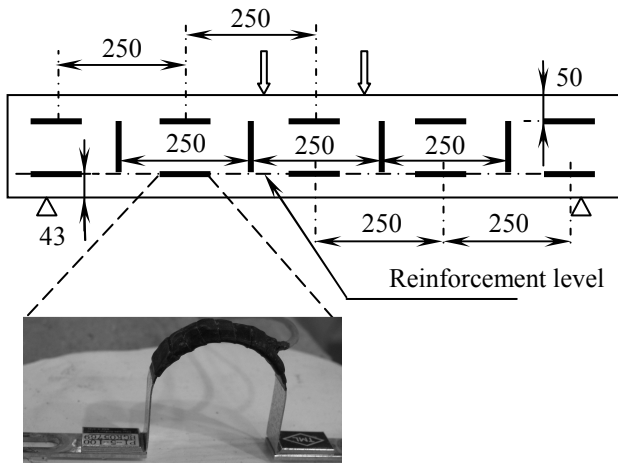


Figure 3. Distribution of PI-5-100 gages on the beam surface.

Table 3. Compressive strength given by Schmidt hammer test $f'_{c,Sch}$.

Concrete Type	$f'_{c,Sch}$ [N/mm ²]
0F80EA	21.1
0F95EA	18.9
05F102EA	19.4
05F110EA	15.9
10F110EA	19.9
10F130EA	15.8

x B) was cast. The beams were designed to fail in shear and had a longitudinal reinforcement ratio: $p_w = 4.3\%$ and a shear span to effective depth ratio: $a/d = 2.71$. The high value for p_w was chosen to ensure shear failure of the beam. More details of the beam geometry and reinforcement are presented in Figure 2. Moreover, as it can be seen from Figure 2, there are no stirrups in the shear span. The reason for such a reinforcement layout is that we wanted to evaluate the shear carrying capacity of the concrete itself without the help of shear reinforcement.

Because expansion agent was never used before to generate random cracks in an RC beam, the decision to measure the strain, both in longitudinal bars and on the concrete surface, was taken. The procedure for strain monitoring is similar to the one described in Toma et al. 2006, with the notable differ-

ence that in this case the concrete surface strain was measured by means of displacement transducers of PI-5-100 type connected to a data logger that recorded the values every 10 minutes. In this way, the evolution of the surface strains in the concrete was monitored very regularly. The location and the layout of the gages are explained Figure 3.

After a curing period of time of 7 days, the beams were subjected to a four-point loading test. The obtained results are presented in the subsequent chapter.

For a better and easier understanding of the discussion on the results in the subsequent chapters, some explanations are necessary regarding the notation of the specimens: in Table 1 and Table 2 “C” stands for the control case, that is the concrete mix containing neither expansion agent nor steel fibers. This is also the reference specimen to which all the other results are compared. All the other specimens’ designations have the following meaning: the first number represents the fiber percentages contained in each specimen and they are 0, for 0% (no fiber), 05 for 0.5% and 10 for 1.0% respectively. They are followed by the letter “F” which stands for fiber. Further on, the second number represents the amount of expansion agent, in kg/m³, that partly replaces the fine aggregates. The expansion agent amount number is followed by the letters “EA” that mean “expansion agent”. Thus, 0F95EA means that the specified mix proportion contains no fiber, 0F, and 95 kg/m³ of expansion agent were used in the mix, 95EA.

5 RESULTS AND DISCUSSION

5.1 Concrete strength

Looking at Table 2, it can be seen that except for the control case C, all the other values for the compressive and tensile strengths are quite uncommon. For this reason, a non-destructive Schmidt hammer test was conducted on the RC beams in order to evaluate the concrete strength in the beams and the obtained values are presented in Table 3.

The big differences between the values given by the uniaxial compression tests on the cylinders and

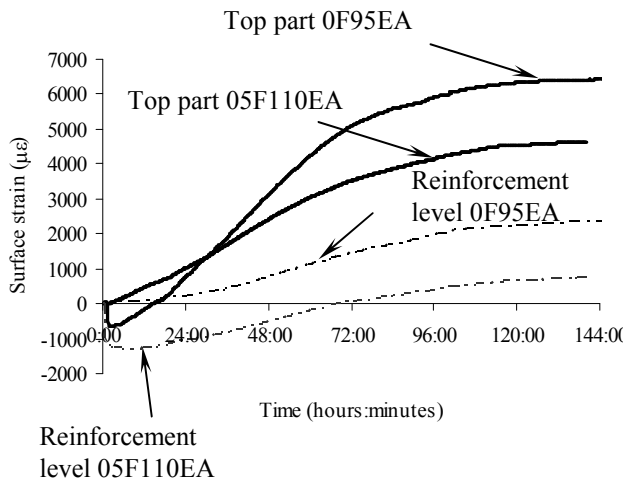


Figure 4. Concrete surface strain history.

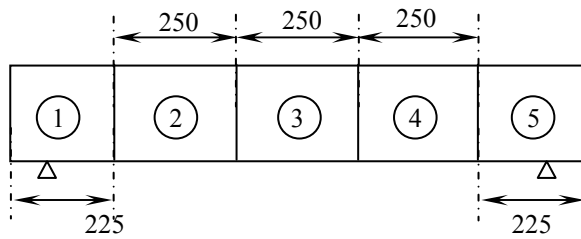


Figure 5. Subdivision of the lateral surface area to evaluate the crack density.

the concrete strength in the beams given by the Schmidt hammer test on the concrete could be explained by the confining effect the reinforcement has on the concrete. This effect cannot be simulated in the cylinders. However, the confining effect of the steel bars cannot justify by itself the large difference between the measured and the expected values. Further studies should be carried out to fully understand the mechanisms behind such high differences.

5.2 Strain history

The steel strain was measured by means of strain gages glued to the reinforcement at the mid-span. The concrete surface strain was measured by means of displacement type strain gages attached to the beam at different locations (Fig. 3). Some of the gages were located on a horizontal line at the reinforcement level whereas others were positioned on a parallel line 50 mm from the top part of the beam. This type of arrangement gives the possibility of better monitoring the deformation of the RC beam during curing.

From the recorded data the strain history during the curing period of time, both in the longitudinal steel and of the concrete surface, is obtained for each specimen. Such an example is shown in Figure 4 for the concrete surface strain.

By looking at Figure 4, it is clear that by adding steel fibers the values for the surface strain both at the top part and at the reinforcement level are getting smaller, even though there is an increase in the amount of expansion agent. Furthermore we can

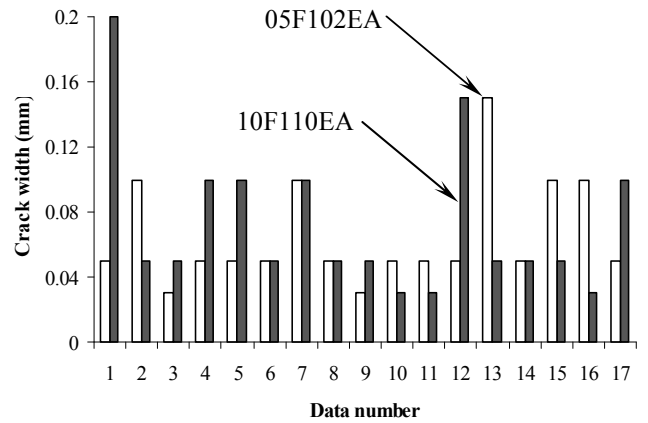


Figure 6. Crack width values for two specimens for area A₂.

conclude that the beam is bent upward during the curing and before being tested. The deformed shape of the RC beams could also be confirmed by visual inspection of the specimens. It is as if an axial force has been applied to the beam, at the reinforcement level, creating some sort of prestressing. Since no axial force was applied to the beam and the deformed shaped was the result of the chemical reactions that took place inside the concrete, this phenomenon may be called chemical prestressing.

The compressive concrete surface strain at the reinforcement level for the 05F110EA could be explained by the combined passive resistance against expansion of both the longitudinal steel bars and the steel fibers. According to Figure 2 there is only a small amount of reinforcement at the upper part of the beam. Consequently, the concrete can expand almost freely. The fiber volume in this case is quite small, 0.5%, to have a significant restraining effect on the concrete. Compared with the 0F95EA case, the occurrence of tensile strains in concrete at the reinforcement level for the beam containing steel fibers happens much later.

5.3 Crack density

Before testing, the specimens were checked for the presence of random cracking, since this was one of the purposes of this research and for which the expansion agent was used. High resolution digital pictures of the beams were taken and later processed by means of special software. After manually tracing all the visible cracks, the total crack length for each area was given by the software.

At the same time, the crack width was measured using a mobile laser crack-width reader with the reading range from 0.01 mm to 2.5 mm, with an increment of 0.05 mm. In order to increase the accuracy of the measured data, the surface of the beam was divided into five areas, Figure 5. The boundary between each individual area was chosen to be the line along which the vertical displacement type

strain gages were placed. For each area readings of the crack width at different locations were taken and the average crack width for that specific area was computed. An example of the values for the crack widths obtained from the measurements is graphically presented in Figure 6 for two beams. The values of the mean crack width of each area are presented in Table 4.

For the purpose of this research, the crack density is defined as the total area of cracks divided by the area of concrete. For each area, the mean crack width is considered. This makes the method more attractive and easier to apply since there is no need to deal with each crack separately; avoiding the debate upon how one defines a crack in the case of random cracking, but with the average value.

Finally, the crack density is computed using the following equation:

$$\Omega_i = \frac{\bar{w}_i \cdot \sum_{j=1}^m L_j}{A_i} \quad (1)$$

in which \bar{w}_i is the average crack width for the area A_i in mm, $\sum_{j=1}^m L_j$ is the total crack length of area A_i given by the software after manual tracing of the cracks, in mm and A_i is the area of concrete, in mm^2 . The index i refers to a specific area the surface of the beam is divided into. The values of the total crack length for each area are summarized in Table 5.

The average crack density factor for the entire specimen can be calculated using Equation 2:

$$\bar{\Omega} = \frac{\sum_{i=1}^n \Omega_i}{n} \quad (2)$$

in which Ω_i is the crack density for i th area and n is the number of areas the concrete surface is divided into. Following the previously mentioned procedure, the crack densities for the specimens that showed random cracks before loading are computed and are presented in Figure 7 as a percentage of the area of concrete together with the random crack pattern for the respective beams.

5.4 Shear carrying capacity

Using expansion agent led to the formation of random cracking and the introduction of steel fibers proved to be effective in limiting the deformation of the RC beams. The next step was to test the specimens for their shear resisting capacity. For this, a four-point loading test was conducted.

Before loading, the ultimate load in shear for each of the specimens was computed by adding the contributions of concrete, steel fibers and chemical prestressing. It all starts from the equation of shear

carrying capacity of a reinforced concrete beam, Equation 3, proposed by Niwa et al. 1986:

$$V_c = 0.2 \cdot f'_c{}^{1/3} \cdot p_w^{1/3} \cdot \left(\frac{d}{1000}\right)^{-1/4} \cdot b_w \cdot d \cdot \left(0.75 + \frac{1.4d}{a}\right) \quad (3)$$

where f'_c is the compressive strength of concrete in N/mm^2 (determined on the concrete from the RC beams by means of the Schmidt hammer test, see Table 3), p_w is the longitudinal reinforcement ratio equal to 4.3%, d is the effective depth, in mm, and b_w is the web thickness, in mm.

As mentioned previously, the use of expansion agent created some sort of chemical prestressing. Its effect was taken into account, according to the standard specifications for concrete structures (JSCE 2002), by the term β_n in the following equation:

$$V_{cp} = V_c \cdot \beta_n \quad (4)$$

where V_c is the shear carrying capacity computed using Equation 3 and β_n is computed by means of the next relationship:

$$\beta_n = 1 + \frac{2 \cdot M_0}{M_u} \quad (5)$$

in which M_u is the ultimate resisting moment of the beam and M_0 is the decompression moment (the bending moment that when applied creates a zero stress in the extreme lower fibers). The procedure for computing the decompression moment is explained in detail in Toma et al. 2006.

Because fibers were also used in this research, their contribution to the shear carrying capacity must be also taken into account. This was done by means of the following empirical equation (Swamy et al. 1993):

$$v = 0.37 \cdot \tau \cdot V_f \cdot \frac{L_f}{d_f} \quad (6)$$

where V_f is the volume of fibers, in %, L_f is the fiber length, in mm, d_f is the fiber diameter, in mm, and τ

Table 4. Mean crack width (mm).

Specimen	Area 1	Area 2	Area 3	Area 4	Area 5
0F95EA	0.15	0.15	0.11	0.15	0.15
05F102EA	0.067	0.065	0.089	0.08	0.082
05F110EA	0.19	0.13	0.08	0.08	0.082
10F110EA	0.08	0.07	0.07	0.09	0.09
10F130EA	0.16	0.19	0.12	0.15	0.14

Table 5. Total crack length (mm).

Specimen	Area 1	Area 2	Area 3	Area 4	Area 5
0F95EA	2900	1560	1110	1650	2940
05F102EA	2000	1450	850	2330	2590
05F110EA	1860	1940	1620	2810	2500
10F110EA	2430	1770	1090	2510	2710
10F130EA	2170	2040	1420	2850	3000

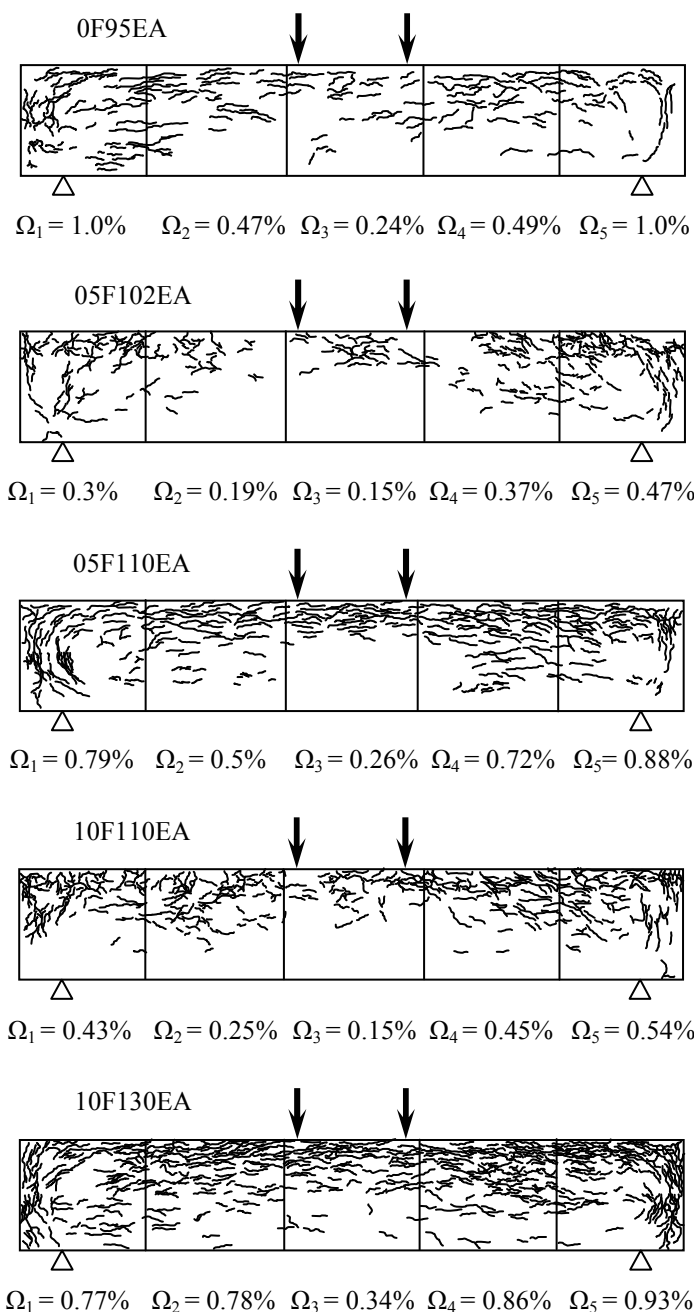


Figure 7. Crack pattern before testing and crack densities for each area as a percentage of the initial area of concrete.

is the bond strength equal to 4.15 N/mm^2 for steel fibers with crimped ends in the absence of any pull-out tests. Equation 6 was shown to provide good accuracy with respect to the experimental data (Cucchiara 2004).

Finally, the shear carrying capacity is computed as:

$$V_{cal} = V_{cp} + v \cdot b_w \cdot d \quad (7)$$

The above-mentioned evaluation procedure was used in previous research works on RC beams, without random pre-cracking, containing both expansion agent and steel fibers and lead to good estimation of the experimental results (Toma et al. 2006).

The predicted peak loads are summarized in Table 6 where they are compared with the values obtained from the loading tests.

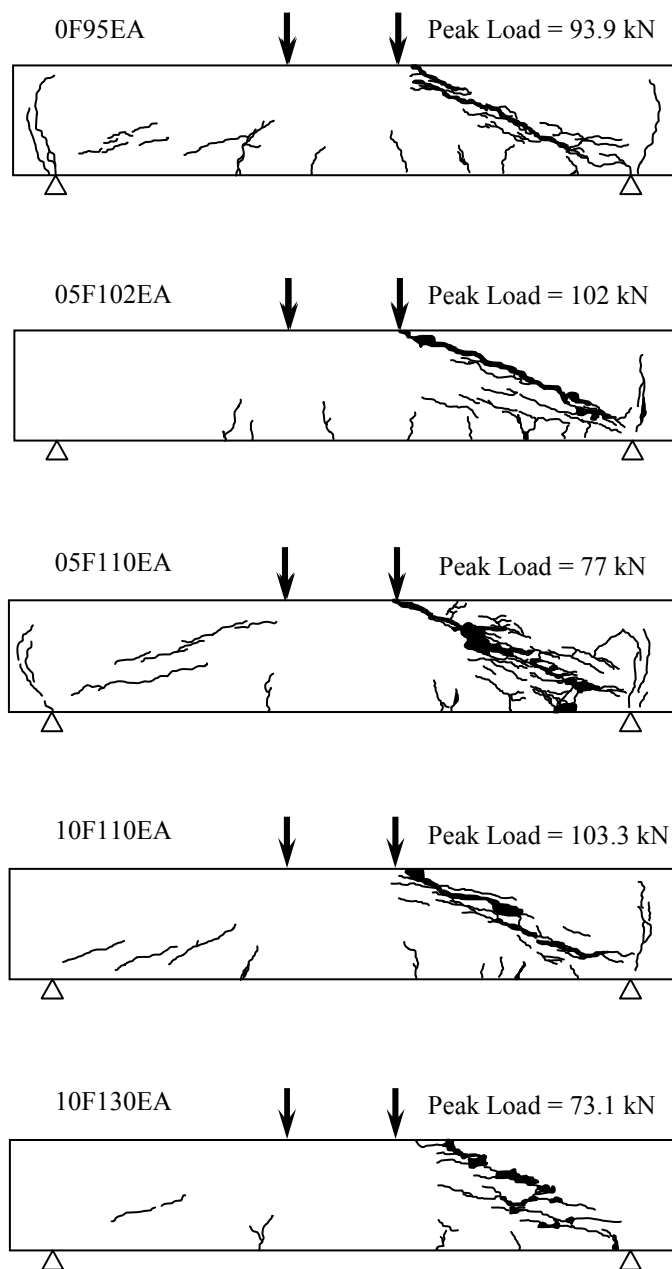


Figure 8. Crack pattern at the onset of shear failure.

Table 6. Calculated results versus experimental results.

Concrete Type	V_{cal} [kN]	V_{exp} [kN]	V_{cal}/V_{exp}
C	69.2	68.5	1.01
0F95EA	111.3	93.9	1.19
05F102EA	93.7	102.0	0.92
05F110EA	134.1	77.0	1.74
10F110EA	115.0	103.3	1.11
10F130EA	130.8	73.1	1.79

By looking at the values of the ratio V_{cal}/V_{exp} in Table 6 it can be seen that the evaluation of the shear carrying capacity of RC beams with random cracks using existing equations leads to an overestimation of the experimental results in most of the cases. This is due to the fact that the existing cracks before load-

ing are not taken into account when evaluating the shear carrying capacity. Summing up, by introducing the unfavorable effect of pre-cracking, the approximation in the evaluation of the ultimate shear capacity would be better.

The crack patterns for each of the tested specimens are presented in Figure 8. A closer look at both Figures 7 and 8 and Table 6 reveals an interesting fact in terms of the location of the shear crack and in terms of the shear carrying capacity. First of all, according to the division of the RC beam surface, areas 2 and 4 are entirely located in the shear span and thus anything occurring in these areas will affect the shear carrying capacity. A comparison between the crack densities Ω_2 and Ω_4 for each of the specimens in Figure 7 shows that in every case $\Omega_2 < \Omega_4$. This means that the shear crack is more likely to happen in the shear span containing area 4 than in the shear span area 2 is located in. According to Figure 8 the failure crack is located in the shear span corresponding to area 4, whose crack density (Ω_4) is larger than that of area 2 (Ω_2).

Moreover, the values of the crack density Ω_4 for each specimen in Figure 7 are somehow related to the shear carrying capacity of each beam. For example, the values of Ω_4 for the specimens 05F110EA and 10F130EA are larger than the value of Ω_4 for 0F95EA and thus the shear carrying capacity of those beams will be smaller than for 0F95EA. This can indeed be seen in Table 6. It is clear that the peak load for 05F102EA will be higher than for 0F95EA because $\Omega_4^{05F102EA} < \Omega_4^{0F95EA}$. However, even though $\Omega_4^{10F110EA} < \Omega_4^{0F95EA}$, see Figure 7, their values are relatively close to one another and so should be their shear carrying capacities. Indeed, the experimental results, presented in Table 6, show an increase in the shear carrying capacity from 93.9 kN for 0F95EA to 103.3 kN for 10F110EA.

6 CONCLUSIONS

Using expansion agent proves to be effective in creating random cracking similar to the cases observed in actual RC members. By changing the amount of expansion agent the random crack pattern before loading can be controlled, in terms of visual observation.

Adding short steel fibers to the concrete mixes has several favorable effects, since steel fibers reduce the surface strains by reducing the mean width of randomly-distributed cracks, increase the deformability of RC members and enhance their shear carrying capacity. However, there are cases when the steel fibers could only increase the deformability of the severely damaged RC beams, with little effect on the peak load.

The notion of crack density is introduced in this research to help for a quantitative representation of

the effect of random cracking. The method is relatively easy to use because it relies on the average crack width and on the total crack length from a specified area of concrete. The high values of the average crack density for the entire specimen lead to lower peak loads for the respective specimens.

The procedure for evaluating the ultimate load in shear for RC beams with random cracks leads to an excessive over-evaluation of the experimental results for the beams that exhibit random cracking before loading. While the addition of steel fibers and the chemical prestress phenomenon that occurred due to the use of expansion agent lead to an increase in the shear carrying capacity, the occurrence of random cracking before loading has a diminishing effect on the peak load. The effect of the latter should be also taken into account. Further tests are necessary (a) to improve the procedure that takes into account the crack density factor; and (b) to quantify in a better way the interaction between the steel fibers and the randomly distributed pre-cracks.

REFERENCES

- Bresler, B. & Scordelis, A.C. 1963. Shear strength of reinforced concrete beams. *ACI Journal*. 60 (1): 51-74.
- Collepari, M., Borsoi, A., Collepari, S., Olagot, J.J.O. & Troli, R. 2005. Effects of shrinkage reducing admixtures in shrinkage compensating concrete under non-wet curing conditions. *Cement & Concrete Composites*, 27: 704-708.
- Cucchiara, C., La Mendola, L & Papia, M. 2004. Effectiveness of stirrups and steel fibers as shear reinforcement. *Cement & Concrete Composites*. 26: 777-786.
- Diamond, S. 1997. Alkali silica reactions – some paradoxes. *Cement & Concrete Composites*. 19: 391-401.
- JSCE. 2002. Standard specifications for concrete structures – structural performance verification, JSCE Guideline for Concrete 3: 25.
- Kreffeld, W. J. & Thurston C. W. 1966. Study on the shear and diagonal tension strength of simply supported reinforced concrete beams. *ACI Journal*. 63 (4): 451-476.
- Niwa, J., Yamada, K., Yokozawa, K. & Okamura, H. 1983. Re-evaluation of the equation for shear strength of reinforced concrete beams without web reinforcement. *Journal of Materials, Concrete Structures and Pavements*, JSCE. 372 (5): 167-176.
- Petersen, K. 1992. Effects of silica fume on alkali-silica expansion in mortar specimens. *Cement & Concrete Research*, 22: 15-22.
- Smaoui, N., Berube, M. A., Fournier, B., Bissonnette, B. & Durand, B. 2005. Effects of alkali addition on the mechanical properties and durability of concrete. *Cement & Concrete Research*, 35: 203-212.
- Swamy, R. N., Jones, R. & Chiam, A.T.P. 1993. Influence of steel fibers on the shear resistance of lightweight concrete T-beams. *ACI Structural Journal*, 90 (1): 103-114.
- Toma, I.O, Miki, T. & Niwa, J. 2006. Influence of steel fibers on the behavior of RC beams with random cracks. *Proceedings of the 10th East Asia-Pacific Conference on Structural Engineering and Construction*, Bangkok, Thailand, Materials, Experimentation, Maintenance and Rehabilitation: 413-418.